EFFECT OF NORMALIZATION ON DUCTILITY AND CORROSION RESISTANCE OF API 5L-X65 PIPE

Yurianto Yurianto[1*] - Aladin Eko Purkuncoro[2] - Padang Yanuar[3] - Taufiqur Rokhman[4]

[1]Metallurgical Engineering Department, Faculty of Manufacturing Technology, UNJANI, Bandung, 40513, Indonesia
[2]Mechanical Engineering Department, Institute of Teknologi Nasional, Malang, 65145, Indonesia
[3]Mechanical Engineering Department, Politeknik Negeri Semarang, Semarang, 50275, Indonesia
[4]Mechanical Engineering Department, Faculty of Engineering, "45" Islamic University, Bekasi 17113, Indonesia

ARTICLE INFO

***Article history*:**
Received: 13.05.2020.
Received in revised form: 16.05.2022.
Accepted: 16.05.2022.

Keywords:
Cracking
Hardening
Heating
Holding
Normalizing

DOI: https://doi.org/10.30765/er.1652

Abstract:

This research studies the effect of normalization on ductility and corrosion resistance of API 5L X65 pipe. Normalization conducted at a temperature of 900 °C with a holding time of 30, 60, 90, 120, and 150 minutes, followed by cooling down to a room temperature by using an external air. Corrosion testing of normalized specimens was performed using seawater as a corrosive environment, -and specimens were also tested for microhardness to determine their mechanical properties. Then, these test specimens were compared with specimens that did not undergo normalization in terms of their microstructure, hardness, and other mechanical properties. The specimens were analyzed by using an Energy Dispersive X-ray (EDX) Spectroscopy to determine the microstructure grain boundary, chemical composition and microcracking of the metal specimens. The results showed that the base metal hardness of API 5L X65 steel pipe fluctuated and tended to decrease. The highest hardness was obtained in specimens without normalizing, and the lowest in normalizing specimens. The highest corrosion rate occurred in specimens without normalizing, and the lowest in specimens with normalizing. Typical corrosion results of seawater on APL 5L-65 pipe are cracking and pitting.

1 Introduction

1.1 Background

With the fast development of technology, the human need for energy also increases. Natural gas is one of the energy sources of concern in this study because it has a lower carbon dioxide (CO2) content than petroleum and coal. Therefore, a pipe length system for the distribution of offshore natural gas is needed. Such a pipe system must have characteristics that are suitable for a corrosive seawater environment. Moreover, the type of steel used for oil and gas pipelines must have high strength and durability under low or normal temperature conditions. In addition, steel for the manufacture of pipes is in sheets that rolled without leaving defects. Salinity is one of the most significant factors causing corrosion in seawater.

The presence of chloride ions in seawater which is aggressive, will form acidic compounds and react with the passive membrane on the alkaline concrete so that the passive membrane will be damaged and the reinforcing steel will corrode. API 5L X65 pipe designed to be the most economical and safe way to transport oil and gas. Many accidents cause by pipe failure caused by corrosion (one of them is seawater corrosion). This corrosion causes plastic deformation, which can change the mechanical properties of this pipe. This corrosive behavior of steel pipe is critical to avoid failure. In the API 5L specification, this pipe was base on ISO standards. Generally, this API 5L X65 ASME Equivalent pipe makes of alloy steel or carbon steel. This pipe is widely used in the petroleum industry because of its low price compared to other

* Corresponding author
E-mail address: yurianto@lecturer.unjani.ac.id

metal and steel categories. Corrosion phenomena cause many 5L-X65 pipe failures; residual stresses play a role in these failures (this stress accelerates chemical erosion)—the residual stress created by the previous pipe rolling process is tensile. Corroded metal becomes brittle (decreased ductility). It is therefore essential to reduce this stress to increase the corrosion resistance of steel. One heat treatment that reduces residual stress is the normalization of heat treatment. Normalizing heat treatment is very suitable for reducing residual stresses in the pipe due to the rolling process in pipe manufacturing.

The stability of the microstructure varies to hold time and becomes more and more stable over time. The formulation of the problem in this research is how the ductility and corrosion resistance after normalizing heat-treated API 5L-65 steel with variations in holding time. The purpose of this study is to evaluate the effect of normalizing heat treatment on the corrosion rate and hardness of API 5L X65 for maritime oil transportation.

The following steps were conducted to achieve the objectives of this study:

a) Before and after the normalization heat treatment, a hardness test was conducted on the API 5L X65 base metal before and after the normalization heat treatment.

b) The corrosion rate of the standard and the normalized specimen was evaluated according to the holding time.

c) Analysis to obtain typical defects produced by seawater corrosion.

Many researchers have investigated the relationship between corrosion and heat treatment. However, there has been no research on ductility and corrosion resistance by stabilizing the structure through the holding period. So herein lies the novelty of this article.

2 Literature review

Low carbon steel must be ductile, which is especially suitable for pipe applications in corrosive environments. As the research results by Neville and Wang, 2009 in **[1]** show that carbon steel with inhibitors is a better economical choice for pipeline material selection under erosion-corrosion conditions, this steel is API 5L-X65 Pipe. These pipes sometimes contain small amounts of niobium (Nb) and vanadium (V) as the main elements of micro-alloy and precipitate hardening. Nb is also relatively corrosion-resistant because V > 0.05% reduces hardenability, all are shown by Hashemi and Mohammadyani [2 & 3]**.** Seawater is a highly abundant and corrosive electrolyte of natural origin. It has a high concentration of salts, mainly in chlorides, and covers approximately 70% of the earth's surface, as shown by Vera et al. [4]. The indentation point on the pipe surface will accelerate corrosion due to the residual stress on the surface.

The pitting corrosion mechanism causes the failure of multiphase natural gas pipelines, as shown in the paper of Mansoori et al. [5]. Fatoba and Akid [6] express that high strength low alloy steel (HSLA) such as American Petroleum Institute (API) grade 5L steel is used in oil and gas structures, e.g., top tension oil enhancer, as it provides superior mechanical properties, corrosion resistance and strength-to-weight ratio than conventional carbon steel. Oliveira et al. express at [7] that the API 5L X65 steel is classified as high resistance and low alloy steel, which presents low carbon content, less than 0.30%, good tenacity, and weldability (easy welding of metal without producing weld defects). Pipelines are the most economical mode of oil transportation and natural gas from the production site to the consumer. Several large pipeline projects can be seen in Datta & Deva [8]**.**

The API 5L X65 pipe is made of cold-rolled API 5L X65 steel plates that joined by submerged arc welding (SAW), using helical junction type. SAW, which is a highly efficient and low-cost traditional welding method, is also an option for improving steels' wear and corrosion resistance, as shown by Oo, et al., Lu, et al. and Wang et al. in **-** [9 - 11]. SAW offers a high amount of deposition weldments, high productivity with cost-effective when compared to any other conventional weld methods as done by Sailender et al. in- [12]. The API 5L X65 pipe is high-strength low steel, low-alloy steel with better mechanical properties and higher corrosion resistance than conventional carbon steel. Steel that has undergone plastic deformation, such as the rolling process, retains permanent tension. The outer and inner surfaces contain tensile and compression residual stresses, respectively. The tension residual stress will trigger a crack. The

steel has cracking sensitivity, which affects its corrosion resistance because of cold cracks, as formulated by Sawhill et al. [13].

$$CE = \%C + \frac{\%Si}{30} + \frac{\%Mn + \%Cu + \%Cr}{20} + \frac{\%Ni}{60} + \frac{\%Mo}{15} + \frac{\%V}{10} + 5\%B \quad (1)$$

CE (carbon equivalent) is the weight percent practical value relating to the combined effects of the various alloying elements used in the manufacture of carbon steel with equivalent amounts of carbon. If CE > 0.35–0.40 (depending on thickness and confinement) it indicates that steel is sensitive to cold cracking on the heat-affected zone (HAZ), except the amount of hydrogen contamination entering the weld pool is reduced. Reheating during normalization can also cause cracking. The tendency of reheat cracking measured by the equation wrote by (1) David et al. [14],

$$C = 10V + 7Nb + 5Ti + Cr + Cu - 2 \quad (2)$$

If C = 0, the steel is sensitive to reheat cracking. The best way to prevent cracking is not to use unexpected alloys as elements P and Nb are identified as triggers of heat cracking of steel, as formulated by Bailey and Jones in [15]. And formulated as,

$$UCS = 230\%C * + 190\%S + 75\%P + 45\%Nb - 12{,}3\%Si - 5{,}4\%Mn - 1 \quad (3)$$

If the carbon in the material is less than 0.08%, then C* = 0.08%. If the carbon content in the material exceeds or equals 0.08%, then C* = carbon contained in the material. Then the UCS crack susceptibility unit > 25 for butt weld. Heat treatment is refine grain size and produce a uniform grain size distribution for pearlite and ferrite. While Yurianto in his paper, after austenitizing finish with enough time, the alloy turns into austenite, and this process is terminated cooling at room temperature [16]. Crack sensitivity also affects the corrosion rate of steel. Dziubinska et al. express that the corrosion rate is affected by structural components [17].

The improvement in the corrosion fatigue life with induced compressive residual stresses is particularly notable in the very high cycle fatigue region, where the allowable working load is increased by a factor of 2.5 compared with the non-overloaded samples, as shown by Okorokov et al. [18]. The HAZ region is more susceptible to corrosion attacks compared to the base metal and weld metal, Tristijanto et al. paper [19]. Corrosive environments (such as seawater) promote the sensitivity of material towards cracking, which facilitates faster corrosion. In making an API 5L X65 pipe, the risk of corrosion occurs when cooling conducts. Water is employed to cool hot-rolled steel intermittently during the rolling process, thus resulting in corrosion as the paper in Liu et al. [20]. Kwok et al., Okayasu et al. and Ren et al express in their paper: roller work must withstand abrasive wear and corrosion at high temperatures to produce hot rolled steel with excellent surface quality as shown in [21 - 23]. Therefore, residual stresses formed under these conditions act as a driver of corrosion, especially at grain boundaries. The measured corrosion rate (CR) of the material tested in mm/year was calculated via the weight loss method and according to standard specimen as wrote by Thorhallsson et al. & ASTM G1-90 in [24 & 25] formulated by:

$$CR = \frac{K \times W}{A \times t \times \rho}(IPY) \quad (4)$$

Where:

K = the corrosion rate constant equal to 8.76×104 mm/year.

W = the mass loss in grams of the tested material with a ± 0.00005 g precision.

A = the exposed surface area in cm^2 of a tested sample.
t = the exposure time in hours, and
ρ = the material density in g/cm^3.

3 Experimental investigation

3.1 Material Used

The material tested and studied is an API 5L X65 pipe welded joint produced by PT. KHI Pipe Industries, Cilegon, Banten. Optical metallography on the API 5L X65 base metal, as shown in Figure 1, using a Nikon Epiphot Metallograph. Microstructural analysis were also performed by using an Optical Emission Spectrometer Machines ARL type 3460 (Switzerland). The chemical element were identified by using an ARL 3460 optical emission spectrometer. Results are shown in Table 1. Hardness was performed using Mcrohardness testers Merk ZWICK Type Zhu (Germany), findings plotted in Figure 6.

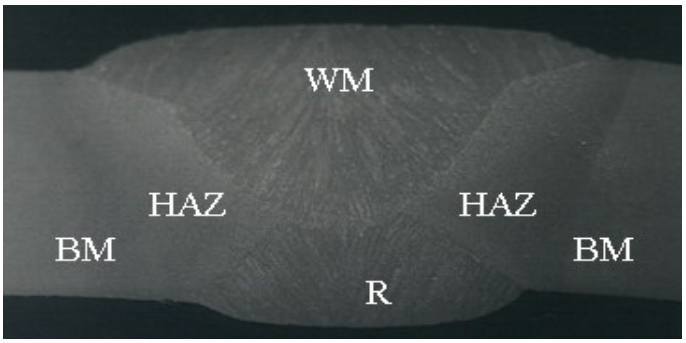

Figure 1. Submerged Arc API 5L-X65 Weld Joint. BM = Base Metal. HAZ = Heat Affected Zone. WM = Weld Metal. R = Root. Welding using V butt joint with roots.

3.2 Method

The materials in this study were the normal specimen which has not yet undergone normalization) and the heat-treated sample (which has undergone heat-treated normalization).

Table 1. Chemical composition of API 5L-X65 Pipe.

Chemical element (%)			
Al	= 0.0435 %	P	= 0.0112 %
C	= 0.0738 %	Pb	= 0.0002 %
Cr	= 0.1693 %	S	= 0.0042 %
Cu	= 0.3185 %	Si	= 0.3716 %
Fe	= 97.0215 %	Sn	= 0.0031 %
Mn	= 1.4158 %	Ti	= 0.0156 %
Mo	= 0.0006 %	V	= 0.4768 %
Nb	= 0.0408 %	W	= 0.0036 %
Ni	= 0.0284 %	Zn	= 0.0015 %

The same corrosive media, namely, seawater, was used for different holding times. The initial conditions are the same for all specimens before and after normalization, which prepared in the same way. In this study, eleven base metal specimens were tested. The same corrosive media, namely, seawater, was used for

different holding times. The initial conditions are the same for all specimens before and after normalization, which were prepared similarly. In this study, eleven base metal specimens were tested.
The specimens were tested by using seawater as a corrosive medium. One sample was connected to a cable (20 cm long) and one end was soldered—the samples before and after corrosion subjected to hardness tests, optical, and electron metallographic observations. The steps of conducting this research are presented in a flowchart, as shown in Figure 2.

The actions taken in the study are as follows:

a) Five test specimens were prepared, and each sample code, as shown in Table 2.
b) LD0-coded specimens were tested for hardness and corrosion rate and subjected to microstructural observations using a scanning electron microscope. With microstructural analysis, the hardness number was obtained.
c) Steps (a) and (b) perform on the LD1, LD2, LD3, LD4, and LD5 specimens.
d) The test data of all specimens discussed, and conclusions were derived.

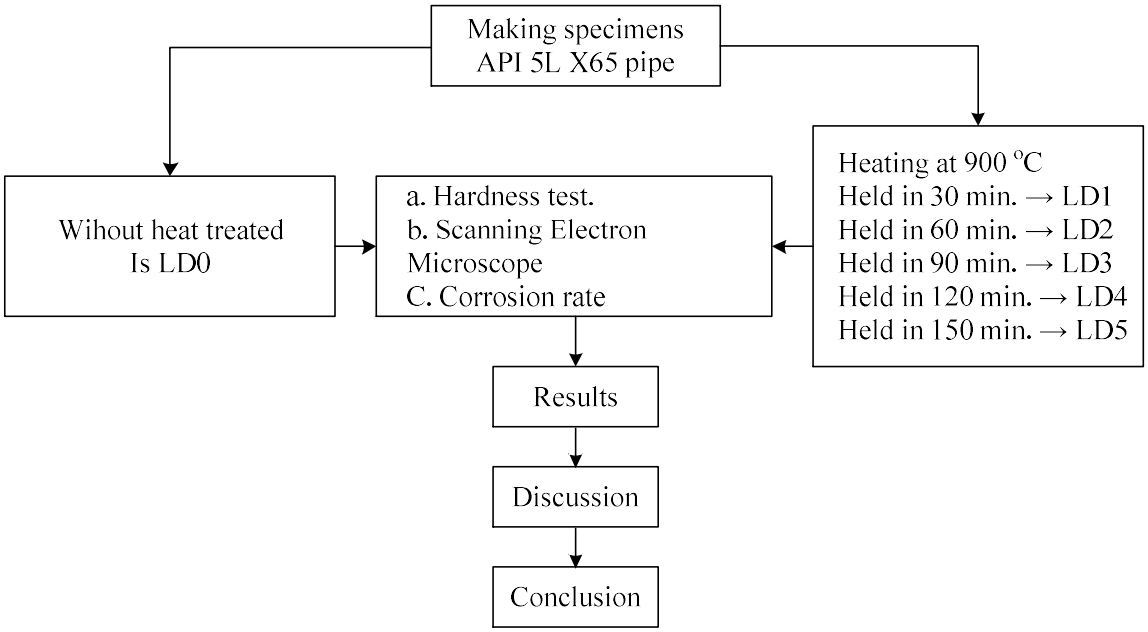

Figure 2. Research flowchart.

Table 2. Pengkodean benda uji.

Code	Normalizing	Holding time
LD0	Untested specimen	None
LD1	900 °C	30 minutes
LD2	900 °C	60 minutes
LD3	900 °C	90 minutes
LD4	900 °C	120 minutes
LD5	900 °C	150 minutes

4 Results and discussion

4.1 Cracking

The base metal was cold-rolled underwent cold rolling in the factory until it reached the plastic limit (when the plates formed), and therefore the base metal contained residual stress. The outer surface of the pipe experienced tensile stress, while the inner surface was subject to residual compression stress. These two stresses make the API 5L X65 pipe sensitive to cold cracks at the fusion boundary in the HAZ of the welding low carbon steel, low alloy, tempered, and tempered steel (on the API 5L X65 pipe). This crack occurs preferentially in alloy-rich bands in the right HAZ and adjacent to the weld interface—the material's sensitivity to cold cracks calculated by using Formula (1). With the elements in Table 1, the CE value equals 0.2296%, meaning it is not sensitive to cold cracking. However, the sensitivity of these cracks remains a concern, mainly if the pipe use below sea level.

The sensitivity to reheat cracking is C = 3.6194%, which is very high. Reheat cracking occurred when welding was performed. Therefore, normalizing heat treatment is needed. Steel that underwent hot cracking with a UCS = 7.232% has a reasonably low crack sensitivity. However, one must minimize corrosion susceptibility in seawater, especially with the residual stress from the previous manufacturing process. API 5L-65. Chemical content of the research specimen shown in Table 1. API 5L X65 pipe welded using SAW; One welding imperfection is point defects on the surface, which trigger the corrosion rate. In addition, a fine crack on the pipe surface (which contains residual tensile stresses resulting from the previous rolling process) is in direct contact with seawater; this condition will also accelerate the corrosion rate. Therefore, the prevention of corrosion in pipelines is a significant concern.

4.2 Percentage reduction of mass

Each specimen was corroded for 2.5 and 5 hours to observe changes in their mass, as shown in Table 3 and Figure 3.

Table 3. Percentage reduction of mass.

Code	2.5 hours		5 hours	
	W2.5 h. (gr)	%	W5 h. (gr)	%
LD0	0.516	16.42	0.771	24.54
LD1	0.306	9.68	0.480	15.18
LD2	0.297	9.75	0.455	14.94
LD3	0.313	10.03	0.507	16.25
LD4	0.270	8.59	0.496	15.78
LD5	0.244	8.32	0.457	15.58

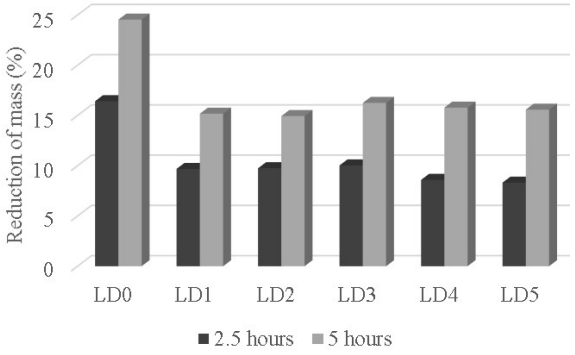

Figure 3. Mass reduction VS duration of corrosion testing.

The outer surface of the pipe has a more significant mass reduction than the inner surface of the tube because the outer surface experienced tensile stress. In contrast, the inner surface experienced residual

compression stress. Holding time has almost no effect on the reduction in specimen mass. The specimens exposed longer in corrosive media exhibited a more significant mass reduction under 2.5 and 5 hours of corrosion during normalization (Figure 3 shows the same graphic shape. The percentage reduction in mass seems to be ultimately constant, which means that the mass did not reduce significantly with increased holding time. The immersion of six test objects showed a tendency to decrease metal mass along with the length of immersion time.

The longer the immersion time, the higher the percentage of mass reduction. Meanwhile, the reduction of mass in the test object due to normalizing heat treatment with variations in holding time almost did not change the reduction in metal mass. At the normalization temperature of 900 °C with various holding times, the reduction in metal mass remains the same. Because the holding time used (30 to 150 min) is the temperature at which the microstructure is microscopically stable. The grain structure remains constant. From these conditions, the change in holding time does not affect the decrease in metal mass, but the longer the immersion time shows, the more significant the reduction in metal mass. However, the LD4 (holding time 120 minutes) and LD5 (holding time 120 minutes) specimens experienced a more significant decrease in mass than the other specimens. It means that holding time that is too long causes a slightly more significant reduction in mass.

4.3 Ductility

The ductility of the specimen before and after corrosion is shown in Table 5 and presented in Figure 4. Ductility is obtained based on the diameter of the Vickers hardness indentation. The smaller the indentation diameter, the higher the hardness (brittle). The elasticity of the specimen before and after exposure to corrosive media was obtained by knowing the average diameter of the Vickers micro-hardness diagonal indentation. Ductility increased significantly after the sample was normalized (with a holding time of 30 minutes) and decreased as the holding time increased to 60 minutes, with increasing holding time (90 minutes). With the use of steel plates for the manufacture of pipes, ductility is preferable to brittle. The ductile pipe that will be damaged provides information before failure occurs. Meanwhile, brittle materials fail immediately without any signs.

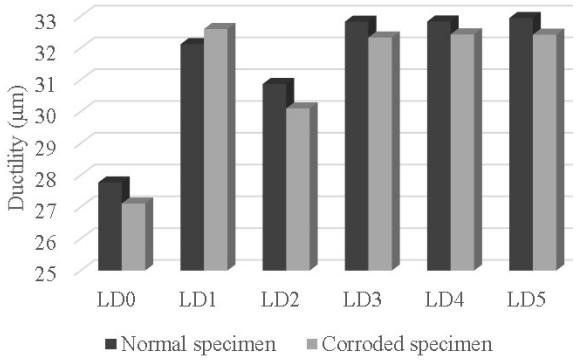

Figure 4. The ductility of normal and corroded specimens.

4.4 Hardness

The standard LD0 specimens have a hardness of 249.77 VHN, which increases to 252.26 VHN after corrosion. The formation of carbide layers after corrosion on the specimen surface causes an increase in hardness. The hardness of the LD1 specimens after corrosion decreased from the standard value of 179.75 VHN to 175.15 VHN. The sample became slightly brittle after corrosion (Table 5 and presented in Figure 5).

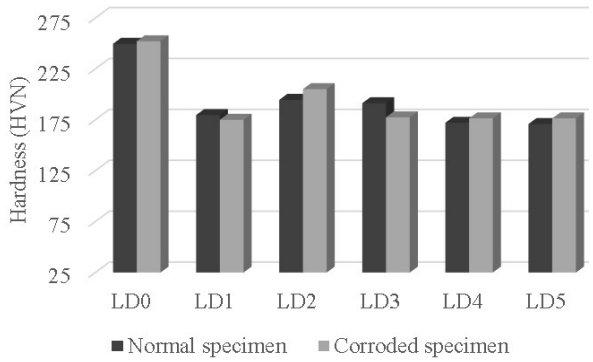

Figure 5. The hardness of normal and corroded specimens.

The hardness of the standard LD2 specimens was 194.65 VHN, which increased to 205.2 VHN. Carbides then formed on the specimen surface, which then became slightly brittle. The standard LD3 samples have a hardness of 191.4 VHN, which can lower to 177.5 VHN, indicating slight fragility. The hardness standard LD4 specimens, 172.15 VHN, increased slightly to 176.45 VHN.

The size of the granular structure increased due to the increased holding time. In the standard LD5 specimens, the hardness decreased slightly compared with the LD4 specimens, 170.9 VHN, and the hardness was 176.45 VHN after corrosion (the same as the LD4 specimens). However, most corroded specimens were slightly more brittle than before being corroded (in this case, using seawater).

4.5 Corrosiion rate

The relation between the corrosion rate and the duration of corrosion shows in Table 4 and Figure 6. Specimens exposed to corrosive media for 2.5 and 5 hours will exhibit show corrosion effects. After exposure to the corrosion medium also showed a slight change in the corrosion rate due to holding time variations. In general, the longer the corrosion rate, the higher the value. For heat-treated specimens, the corrosion rate decreased. This decrease in corrosion rate is due to the release of the residual stress (the rolling process process during pipe loading) by normalizing heat treatment. The residual stress at the pipe surface is the tensile stress. Figure 4 shows that the use of holding longer does not affect the corrosion rate. Temperature 900 °C has a powerful residual stress release effect.

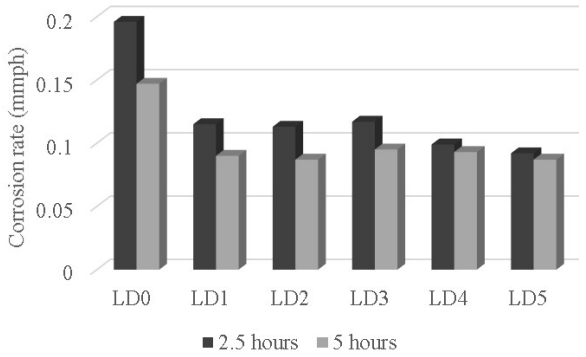

Figure 6. Corrosion rate vs duration of corrosion testing.

4.6 Microstructural analysis

The results of the microstructure analysis are graphically presented in Figures 7 – 12. In Figure 7a, normal specimen LD0 shows that most of the structure is ferrite with less pearlite, and the hardness of ferrite is lower than that of pearlite. It appears that the fine grain structure indicates the ductile nature of the

material resulting in a reliable APL 5L-X65 pipe. However, under normal circumstances, it also contains residual stresses resulting from rolling. In addition, there are also some tiny defects in the form of point defects, these minor defects are stresses, and these small defects will trigger corrosion.

This pipe containing small amounts of Nb have corrosion resistance, and V as and precipitate hardening. Figure 7b shows a corroded specimen with seawater as the medium. When the surfaces corroded, valleys are formed due to the stretching of the grain boundaries by the corrosion medium due to the residual tensile stress (valley is the trigger for metal failure). The corrosion process produces corrosion flowers in the valley. If this incident is continuous (plus fluid pressure from inside the pipe), there will be damage in the form of a tear in the pipe. Figure 8a shows grain refinement due to heating at 900 °C with a holding time of 30 minutes. In this heating, residual stress reduction occurs. Due to the fine structure, the ductility and strength increased.

Table 4. Corrosion rate vs duration of corrosion testing.

Spec. Code	2.5 hours					5 hours				
	W (gr)	A (in^2)	A (mm^2)	CR (IPY)	CR (mmph)	W (gr)	A (in^2)	A (mm^2)	CR (IPY)	CR (mmph)
LD0	0.516	0.207	27.644	67.62	0.196	0.771	0.207	27.644	50.52	0.147
LD1	0.306	0.210	28.452	39.54	0.115	0.480	0.210	28.452	31.02	0.090
LD2	0.297	0.207	27.644	39.01	0.113	0.455	0.207	27.644	29.88	0.087
LD3	0.313	0.210	28.452	40.49	0.117	0.507	0.210	28.452	32.79	0.095
LD4	0.270	0.207	27.644	34.14	0.099	0.486	0.207	27.644	31.91	0.093
LD5	0.244	0.208	27.912	31.84	0.092	0.455	0.208	27.912	29.69	0.087

Table 5. Ductility for normal specimen.

Spec. Code	Normal specimen					Corroded specimen				
	D_1 (μm)	D_2 (μm)	D (μm)	D_{mean} (μm)	Hard	D_1 (μm)	D_2 (μm)	D (μm)	D_{mean} (μm)	Hard (VHN)
LD0	28.67	26.74	27.701	27.77	249.77	27.32	27.32	27.32	27.11	252.26
	28.26	27.41	27.835			28.24	25.57	26.905		
LD1	34.07	30.49	32.28	32.12	179.75	30.93	31.95	31.44	32.60	175.15
	32.81	31.12	31.965			33.39	34.12	33.755		
LD2	31.67	30.11	30.89	30.87	194.65	29.49	28.98	29.235	30.10	205.2
	31.75	29.92	30.84			31.97	29.94	30.955		
LD3	30.08	30.16	30.12	32.83	191.4	32.9	32.47	32.685	32.33	177.5
	33.34	31.15	32.25			31.47	32.47	31.97		
LD4	31.95	33.50	32.725	32.835	172.15	32.86	30.91	31.885	32.43	176.45
	32.47	33.38	32.925			32.56	33.4	32.98		
LD5	33.14	32.95	33.045	32.945	170.9	34.31	29.77	32.04	32.42	176.45
	33.65	32.04	32.845			33.97	31.63	32.8		

Small grains at the grain boundaries indicate grain growth. Figure 8b shows that the corrosion interest is getting bigger. Corrosion results have tiny cracks and pitting, in addition to inclusions. Long-term deposition of corrosion products and descaling will trap small amounts of moisture in the product oil, creating conditions for corrosion and causing sub-scale corrosion, as shown by Wang et al. in [26]. Figure 9a shows a slightly larger grain (as compared to LD2). Due to the long holding time, the grain structure slightly enlarged and decreasing the ductility. Here the grain growth appears to be getting more significant at the grain boundaries with a holding time of 60 minutes. Figure 9b shows white lump-like cotton due to corrosion and slightly eroded the metal surface underneath. The boundary surface between the lump and the metal is a zone that is prone to cracking. In addition, the corrosion results on the LD2 specimen began to show small cracks around the white lumps and would grow during corrosion. Cracks play an essential

role in metal decay. Figure 10a shows the larger grain structure (LD3 specimen). At 90 minutes, holding time allows moisture to evaporate. Ductility decreased compared to LD1 and LD2 specimens. In the picture, it appears that grain growth occurs (at grain boundaries). Here the grain growth is more significant with increasing holding time (90 minutes), especially at the branching of the three-grain boundaries. Figure 10b shows the corroded lumps have solidified, and the crack intensity looks sharper (as indicated by the arrows). Corrosion products such as inclusions and cracks will accelerate corrosion. Especially with coarser grains, it will accelerate the corrosion rate, especially at the grain boundaries. Figure 10b shows the corroded lumps have solidified, and the crack intensity looks sharper (as indicated by the arrows). Corrosion products uch as inclusions and cracks will accelerate corrosion. Especially with coarser grains, it will accelerate the corrosion rate, especially at the grain boundaries.

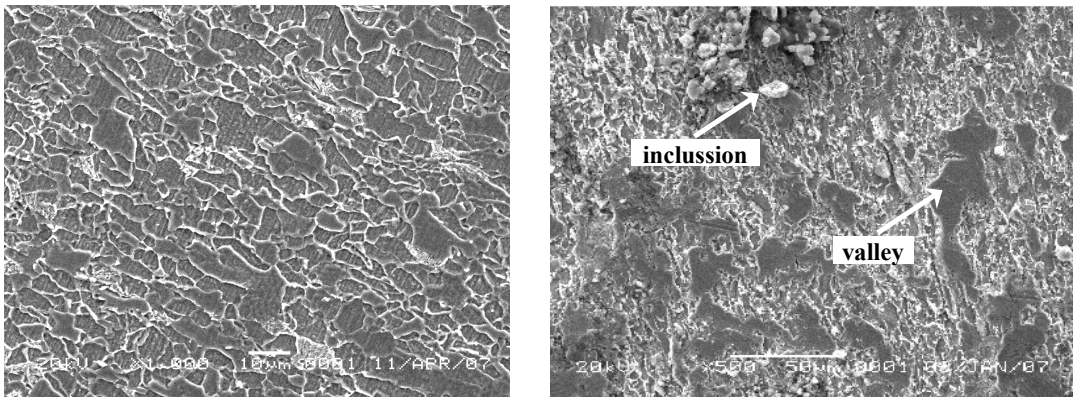

(a) Without corrosion, magnified 1000× *(b) Corroded specimen, magnified 500×*

Figure 7. Scanning Electron Microscope on LD0 specimens.

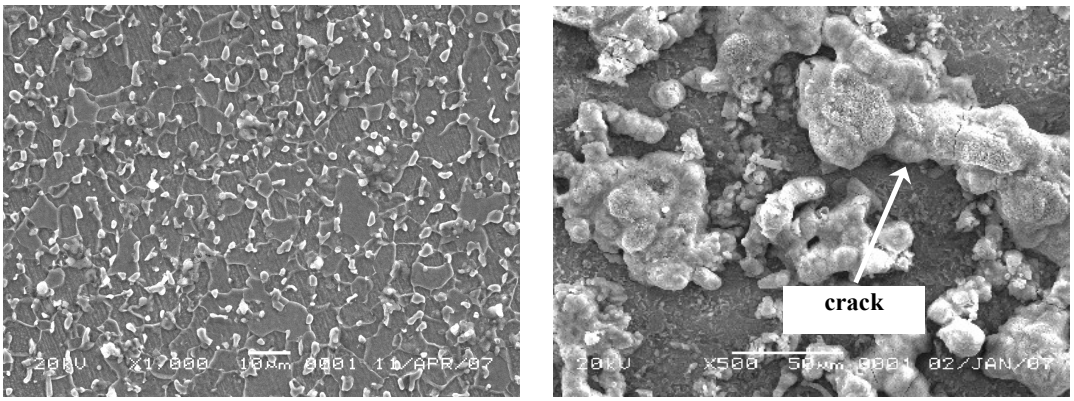

(a) Without corrosion, magnified 1000 × *(b) Corroded specimen, magnified 500×*

Figure 8. Scanning Electron Microscope on LD1 specimens.

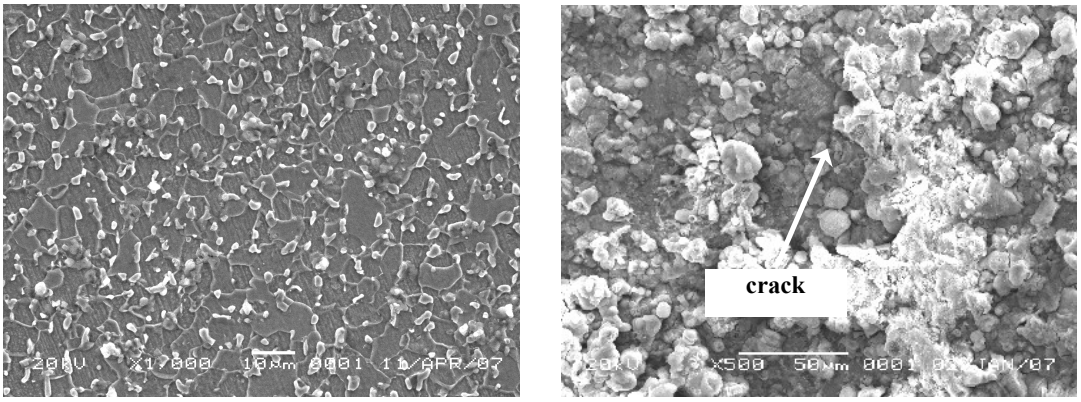

(a) Normal specimen, magnified 1000 × *(b) Corroded specimen, magnified 500×*

Figure 9. Scanning Electron Microscope on LD2.

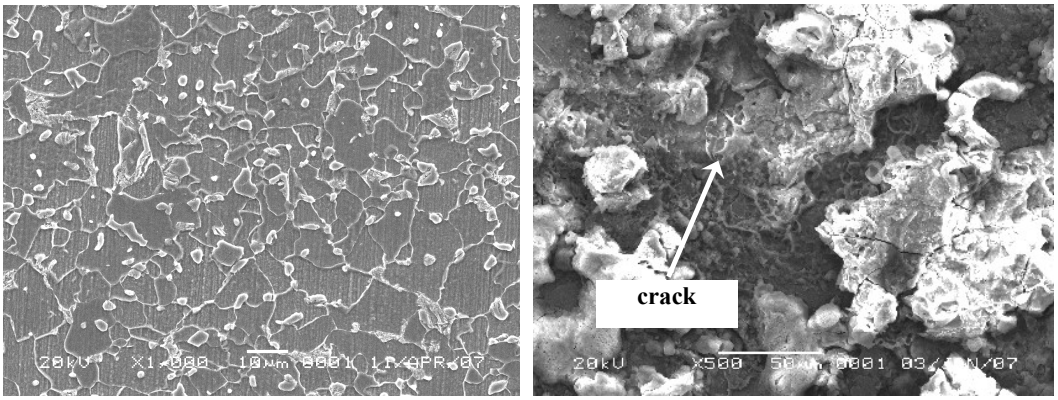

(a) Normal specimen, magnified 1000 × *(b) Corroded specimen, magnified 500×*

Figure 10. Scanning Electron Microscope on LD3 specimens.

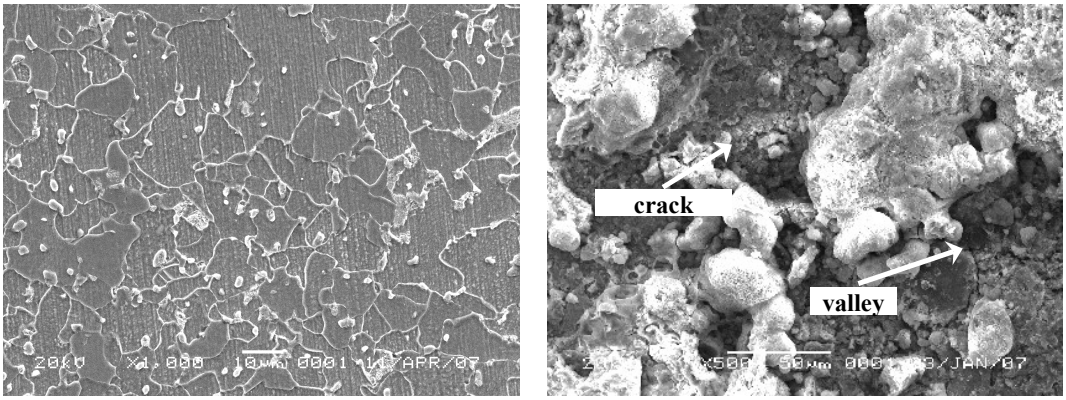

(a) Normal l specimen, magnified 1000 × *(b) Corroded specimen, magnified 500×*

Figure 11. Scanning Electron Microscope on LD4 specimens.

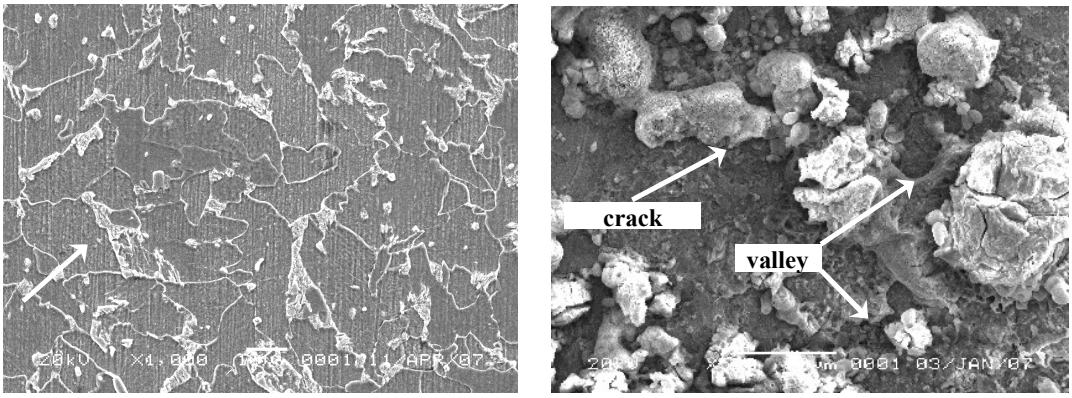

(a) Normal specimen, magnified 1000 × *(b) Corroded specimen, magnified 500×*

Figure 12. Scanning Electron Microscope on LD5 specimens.

Figure 11a shows the coarser grain structure. It is due to the use of a more extended holding (i.e., 120 minutes) so that the residual stress reduces the crack susceptibility. In the picture, it appears that the growth of the grain structure (in the picture, it appears at the grain boundaries) is getting bigger. Figure 11b shows the LD4 corroded specimen. The picture looks like a white lump like cotton shows a crack between the white lump and the metal surface. Pitting appears more considerable, as do the cracks between the white lumps and the metal surface. Figure 12a shows the LD5 specimen where the grain structure is larger than the LD0, LD1, LD2, and LD3 specimens. Using a holding time of 150 minutes resulted in grain growth, which resulted in a more prominent grain structure. Figure 12b shows cracks and steep valleys as corrosion. White lumps with cracks underneath.

4 Conclusion

The hardness value obtained by the Vickers hardness test conducted on the API 5L X65 pipe is metal without normalization (LD0) is 249.77 VHN. For corroded specimens, LD4 and LD5 are the same, namely 176.45 VHN. Corrosion test on API 5L X65 base metal pipe showed the highest corrosion rate occurred in the standard specimen. The corrosion rate decreased significantly and slightly fluctuated in the corroded sample, with a value much lower than the untested specimen. Typical corrosion on APL 5L-65 pipe are produces cracking and pitting. The most significant corrosion effect occurs on specimens subjected to normalizing heat treatment.

References

[1] A.Neville, C. Wang: *Erosion–corrosion of engineering steels—Can it be managed by use of chemicals?,* Wear 267 (2009) 2018–2026.

[2] S.H. Hashemi, D. *Mohammadyani: Characteri-sation of weldment hardness, impact energy and microstructure in API X65 steel*, International Journal of Pressure Vessels and Piping 98 (2012) 8-15.

[3] J.R. Davis, 2001, Alloying Understanding The Basics, ISBN: 0-87170-744-6, ASM International Materials Park, OH 44073-0002.

[4] Rosa Vera, Fabrizio Vinciguerra, Margarita Bagnara: *Comparative Study of the Behavior of API 5L-X65 Grade Steel and ASTM A53-B Grade Steel against Corrosion in Seawater,* Int. J. Electrochem. Sci., 10 (2015) 6187 – 6198.

[5] Hamed Mansoori, Reza Mirzaee, Feridun Esma-eilzadeh, Arash Vojood, Alireza Soltan Dowrani*, Pitting corrosion failure analysis of a wet gas pipeline,* Engineering Failure Analysis 82 (2017) 16–25.

[6] Olusegun Fatoba, Robert Akid: *Uniaxial cyclic elasto-plastic deformation and fatigue failure of API-5L X65 steel under various loading conditions*, Theoretical and Applied Fracture Mechanics 94 (2018) 147–159.

[7] Mariana Cristina de Oliveira, Rodrigo Eduardo Monzon Figueredo, Heloisa Andréa Acciari, Norberto Codaro: Corrosion behavior of API 5L X65 steel subject plastic to deformation, J. MATER RES TECHNOL. 201 8;7(3): 314–318.

[8] Datta, R., Deva, A.: *An Investigation into the Failure of API 5L X-46 Grade ERW Linepipes*, Practical Failure Analysis, 2 (2002), 2, 60-62.

[9] Oo, H. Z, Muangjunburee, P.: *Wear behaviur of hardfacing on 3.5% chromium cast steel by submerged arc welding*, Materials Today, 5 (201), 9281–9289.

[10] Lu, S. P., Kwon, O. Y., Kim, T. B., Kim, K.H.: *Microstructure and wear property of FeMn-Cr-M-V alloy cladding by submerged arc welding*, Journal Material Process Technology, 147 (2004), 191–196.

[11] Wang, X. Y., Wang, J. H., Gao, Z. M., Xi, D. H., Hu, W. B.: *Tempering effects on the micro-structure and properties of submerged arc surfacing layers of H13 steel*, Journal Material Process Technology, 269 (2019), 26–34.

[12] Sailender, M., Suresh, R., Reddy, G., Venkatesh, S.: *Prediction and Comparison of the Dilution and Heat Affected Zone in Submerged Arc Welding of Low Carbon Alloy Steel Joints*, Measurement (2019), 701084.

[13] Sawhill, J., Baker, M. Jr., Howe, P.: *Hydrogen-assisted cracking in high-strength pipe-line steels*, Welding Journal, 7 (1986), 175-s–183-s.

[14] David, L. O., Thomas, A. S., Stephen, Liu, Glen, R. E.: *Welding, Brazing, and Soldering*, ASM Handbook, Vol. 6, ASM International, Ohio, 1993.

[15] Bailey, N., F. R. Coe, T. G. Googh, P. H. M. Hart, N. Jenkins and R. J. Pargetter, (1973), Welding steels without hydrogen cracking, Abington Publishing and ASM International.

[16] Yurianto, Y.: *HAZ crack sensitivity of API 5L-X65 pipe weld joint)*, Semnas Rekayasa Manufaktur dan Industri Teknik Mesin, Semarang, Indonesia, 2005, 150-155.

[17] Dziubinska, A., Ostapiuk, M., Siemionek, E.: *Corrosion resistance of Mg4AlZn alloy aircraft brackets produced by new forging methods*, Procedia Manufacturing, 15 (2018), 419–426.

[18] Okorokov, V., Morgantini, M., Gorash, Y., Comlekci, T., Mackenzie, D., van Rijswick, R.: *Corrosion fatigue of low carbon steel under com-pressive residual stress field*, Procedia Engineering, 213 (2018), 674–681.

[19] Tristijanto, H., Ilman, M. N. Iswanto, P. T.: *Corrosion Inhibition of Welded of X – 52 Steel Pipelines by Sodium Molybdate in 3.5% NaCl Solution*, Egyptian Journal of Petroleum, https://doi. org/10. 1016/j.ejpe. 2020.02.001.

[20] Liu, Z., Fu, P., Zhao, J., Ji, F., Zhang, Y., Nagaumi, H., Wang, X., Zhao, Y., Jia, P., Li., W.: *Corrosion and high-temperature tribological behavior of carbon steel claddings by additive manufacturing technology*, Surface & Coating Technology, 384 (2020), 125325.

[21] Kwok, C. T., Cheng, F. T., Man, H. C.: *Micro-structure and corrosion behavior of laser surface-melted high-speed steels*, Surface & Coating Technology, 202 (2007), 336–348.

[22] Okayasu, M., Wu, S., H.: *Effects of oxide scale on the corrosion and mechanical properties for a highspeed steel and a graphite cast iron*, Oxide of Metals, 87 (2017), 159–178.

[23] Ren, X. Y., Fu, H. G., Xing, J. D., Yi, Y. L.: *Research on high-temperature dry sliding friction wear behavior of Ca-Ti modified high boron high speed steel*, Tribology International, 132 (2019), 165–176.

[24] Thorhallsson, A. I., Stefansson, A., Kovalov, D., Karlsdottir, S. N.,: *Corrosion testing of materials in simulated superheated geothermal environment,* Corrosion Science, 168 (2020), 108584.

[25] ASTM International, ASTM G1-90: Standard Practice for Preparing, Cleaning, and Evaluating Corrosion Test Specimens, (2017), p. 3 https:// www.astm.org/Standards/G1.

[26] Zhengquan Wang, Ziyang Zhou, Weichen Xu, Lihui Yang, Binbin Zhang, Yantao Li: *Study on inner corrosion behavior of high strength product oil pipelines*, Engineering Failure Analysis 115 (2020) 104659.